SUPPLEMENTARY NEUTRON-FLUX CALCULATIONS FOR THE ORNL POOL CRITICAL ASSEMBLY PRESSURE VESSEL FACILITY*

CONF-820321--9

DE82 009135

P. J. Maudlin
Los Alamos Scientific Laboratory
Los Alamos, New Mexico, USA
R. E. Maerker
Oak Ridge National Laboratory
Oak Ridge, Tennessee, USA

ABSTRACT

A three-dimensional Monte Carlo calculation using the MORSE code was performed to validate a procedure previously adopted in the ORNL discrete ordinate analysis of measurements made in the ORNL Pool Critical Assembly Pressure Vessel Facility. The results of these flux calculations agree, within statistical uncertainties of about 5%, with those obtained from a discrete ordinate analysis employing the same procedure. This study therefore concludes that the procedure for combining several one-and two-dimensional discrete ordinate calculations into a three-dimensional flux is sufficiently accurate that it does not account for the existing discrepancies observed between calculations and measurements in this facility.

INTRODUCTION

The Pool Critical Assembly Pressure Vessel Facility (PCA-PVF) was instituted to serve as a benchmark facility for validating calculational procedures in predicting neutron fluences in reactor pressure vessels for estimation of damage.[1] A description of the various calculations carried out for the PCA-PVF by an international group of analysts has been documented.[2,3] An underprediction (10 to 20%) seems to persist throughout a majority of the calculation-versus-experimental comparisons, and the source of this discrepancy is presently a point of speculation and controversy.

With one exception, all the analysts used one-and two-dimensional discrete ordinate transport methods and combined them in some way. The one exception used a continuous energy forward Monte Carlo method with importance sampling and biasing to perform a three dimensional calculation, but unfortunately the results had fairly large statistical uncertainties at times.[2,3]

*This work was sponsored by the Electric Power Research Institute under research project 1399-1, under Union Carbide Corporation contract W-7405-eng-26 with U.S. Department of Energy.

A tenable procedure first suggested by Combustion Engineering[2,3] and adopted by Oak Ridge[2-6] for scaling the discrete ordinate calculations may be summarized by the following flux synthesis equation:

$$\phi(x,y,z,E,\vec{\Omega}) \cong \phi(x,y,E,\vec{\Omega})\phi(y,z,E,\vec{\Omega})/\phi(y,E,\vec{\Omega}), \quad (1)$$

or, more conveniently,

$$\phi_{XYZ} \cong \phi_{XY}\,[\phi_{YZ}/\phi_{Y}] \quad (2)$$

where in the present application the accuracy of this approximation needs only to be evaluated at locations along the y-axis (i.e., for x=z=0 in Fig. 2 appearing in next section). Equation (2) states that a three-dimensional flux, ϕ_{XYZ}, can be constructed from two two-dimensional calculations, ϕ_{XY} and ϕ_{YZ}, and a one-dimensional calculation, ϕ_{Y}, by simply scaling the ϕ_{XY} calculation by a properly normalized z-correction term appearing in the brackets. The ϕ_{XY}, ϕ_{YZ}, and ϕ_{Y} calculations have geometry of infinite extent in the z-direction, x-direction and x,z-directions respectively. An inspection of Eq.(2) shows that the assumption underlying this particular flux synthesis is that the vertical (i.e.,z) flux profiles are the same for all x locations, i.e., the three-dimensional fluxes are separable in x and z.

In the PCA-PVF calculations, the source per unit height for the midplane XY calculation is normalized in such a way that when integrated over x, y, and z yields a value of unity (i.e., there is one fission neutron in the core). The effects of finite z essentially arise as a result of a source limited to the height of the core and with a measured cosine distribution peaking in the vicinity of the centerline. The normalization of the source distribution in z for the ϕ_{YZ} calculation relative to the source per unit height for the ϕ_{Y} calculation, with the ϕ_{XY} source the midplane source as described above, must be set equal to the ratio of the average to the midplane values as pictured in Fig. 1.

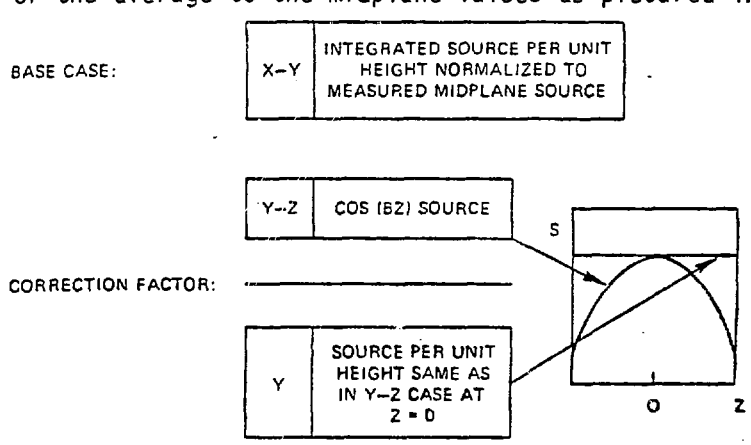

Fig. 1. Correcting Two-Dimensional Calculations for Finite Core Height and Measured Fission Density Distribution.

The object of this work is to evaluate the accuracy of Eq. (2) by calculating directly the three-dimensional flux ϕ_{XYZ} via a Monte Carlo transport code and to compare these results with the flux approximated by the right hand side of Eq. (2). For this purpose, the multigroup Monte Carlo code MORSE[7] was used to calculate ϕ_{XYZ} and the DOT-IV[8] discrete ordinates code was used to calculate ϕ_{XY}, ϕ_{YZ}, and ϕ_{Y}.

PHYSICAL DESCRIPTION OF THE PCA-PVF

The PCA-PVF was designed to simulate within intensity constraints the geometry and arrangement of materials that exist within a commercial pressurized water reactor pressure vessel. The geometry illustrated in Fig. 2 shows the locations of the PCA core, aluminum window (in analogy to the geometry of the Poolside Facility (PSF) in which high intensity measurements using the ORR were also performed), appropriate water gaps, and steel slabs representing the thermal shield and pressure vessel wall. This geometry is a slight simplification of the actual configuration, but should not compromise the present analysis. Values of 8.4 and 6.7 cm. respectively for the large water gap dimensions in Fig. 2 were used in this analysis. This "8/7 configuration" was chosen over the "12/13 configuration," which was more extensively measured, to reduce the statistical uncertainties in the MORSE calculations.

A reflective boundary condition exists on the left face of the core (i.e., the xz plane at y=0), and a vacuum boundary condition exists on the right face of the pressure vessel in Fig. 2 (i.e., the xz plane at y=66.7 cm). All remaining slab faces are reflected with water.

Seven neutron flux detectors designated D1 through D7, with coordinates as shown in Fig. 2, include all the locations along the y-axis where measurements were made along with the additional ones D2 and D4.

The spatial zones in Fig. 2 are identified by the cross-section medium numbers M1 through M8. In the pressure vessel there are three sets of cross sections, each weighted over a different region of the carbon steel with fluxes from a one-dimensional discrete ordinates calculation. Similarly, the two large water gaps have slightly different cross sections.

The fixed neutron source distribution has been documented,[2,3] and for the present purposes can be approximated as

$$S_{XYZ}(x,y,z) = S_{XY}(x,y) \cos(.0442z), \quad -30\text{cm} \leq z \leq 30\text{cm}, \tag{3}$$

where $S_{XY}(x,y)$ has quarter core symmetry and appears in Fig. 3. The average to centerline value for the z distribution in Eq. (3), which is the relative normalization of the ϕ_{YZ} to ϕ_{Y} calculations, becomes

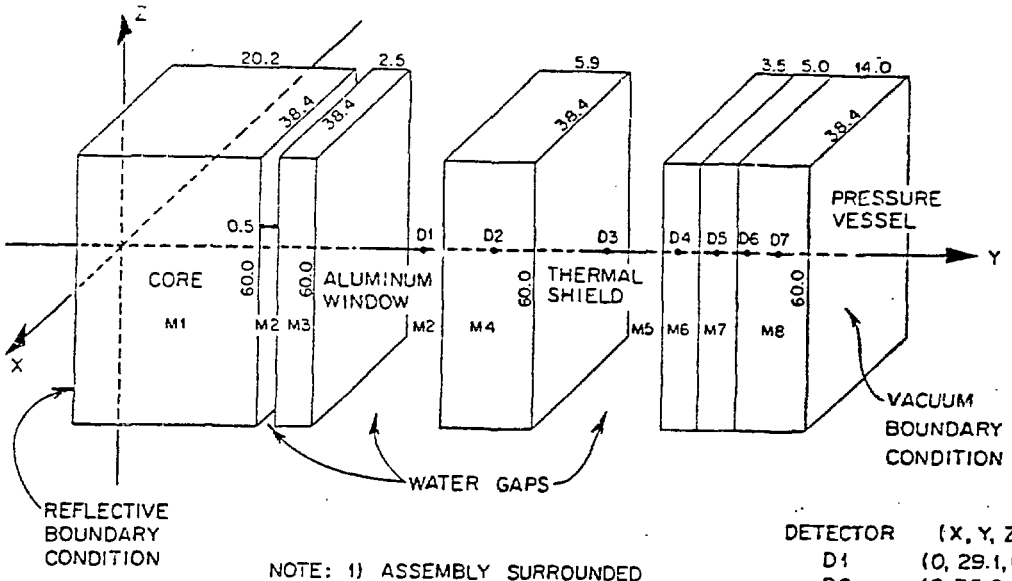

NOTE: 1) ASSEMBLY SURROUNDED BY WATER
2) ALL DIMENSIONS IN cm
3) DRAWING NOT TO SCALE

DETECTOR	(X, Y, Z)
D1	(0, 29.1, 0)
D2	(0, 35.0, 0)
D3	(0, 40.9, 0)
D4	(0, 45.7, 0)
D5	(0, 50.6, 0)
D6	(0, 55.8, 0)
D7	(0, 61.2, 0)

Fig. 2. Modeling Geometry for the Pool Critical Assembly Pressure Vessel Facility. For the 8/7 Configuration, the two Large Water Gaps are 8.4-and 6.7-cm. wide respectively.

ORNL-DWG 80-20108

x (cm)	y (cm)																				
18.8	0	1.79	1.82	1.82	1.82	1.69	1.69	1.69	1.69	1.69	1.69	1.49	1.49	1.49	1.32	1.32	1.12	1.12	1.12	1.12	0.99	0.99	0.99
17.7	1.3	1.79	1.82	1.82	1.82	1.69	1.69	1.69	1.69	1.69	1.69	1.49	1.49	1.49	1.32	1.32	1.12	1.12	1.12	1.12	0.99	0.99	0.99
16.6	2.2	1.70	1.70	1.70	1.67	1.59	1.59	1.55	1.55	1.55	1.55	1.37	1.37	1.37	1.22	1.22	1.05	1.05	1.05	1.05	0.96	0.96	0.96
15.1	3.1	1.70	1.70	1.70	1.67	1.59	1.59	1.55	1.55	1.55	1.55	1.37	1.37	1.37	1.22	1.22	1.05	1.05	1.05	1.05	0.96	0.96	0.96
14.3	4.0	1.87	1.87	1.87	1.87	1.86	1.86	1.91	1.91	1.91	1.91	1.69	1.69	1.69	1.48	1.48	1.16	1.16	1.16	1.16	1.11	1.11	1.11
12.1	5.1	0	0	0	0	0	0	0	0	0	0	0	0	0	0	0	0	0	0	0	0	0	0
11.0	6.2	2.66	2.74	2.74	2.74	2.80	2.80	0	0	0	0	0	2.19	2.19	1.69	1.69	1.35	1.35	1.35	1.35	1.24	1.24	1.24
8.9	7.0	2.66	2.91	2.91	2.91	3.07	3.07	0	0	0	0	0	2.38	2.38	1.79	1.79	1.42	1.42	1.42	1.42	1.29	1.29	1.29
6.5	7.8	2.96	3.07	3.07	3.07	3.26	3.26	0	0	0	0	0	2.50	2.50	1.94	1.94	1.50	1.50	1.50	1.50	1.39	1.39	1.39
4.4	8.6	0	0	0	0	0	0	0	0	0	0	0	0	0	0	0	0	0	0	0	0	0	0
3.3	9.4	2.50	2.53	2.53	2.53	2.51	2.51	2.58	2.58	2.58	2.58	2.21	2.21	2.21	1.94	1.94	1.57	1.57	1.57	1.57	1.46	1.46	1.46
1.2	10.3	2.54	2.57	2.57	2.57	2.40	2.40	2.32	2.32	2.32	2.32	2.03	2.03	2.03	1.85	1.85	1.56	1.56	1.56	1.56	1.41	1.41	1.41
0	11.2																						
	12.1																						
	13.2																						
	14.3																						
	15.1																						
	15.9																						
	16.7																						
	17.5																						
	18.4 - 19.3																						
	20.2																						

Fig. 3. Quarter Core Midplane Fission Neutron Source Distribution in Units of 10^{-5} neutrons per second per $cm.^3$

$$\frac{\overline{S}_{YZ}}{S_Y} = \frac{\int_{-30}^{30} \cos(.0442z)dz}{\int_{-30}^{30} dz} = 0.7317. \quad (4)$$

CALCULATIONAL DETAILS

An adequate comparison of the results from the two methods should not be strongly influenced by the particular cross section sets used, as long as they are the same in each method. Consequently, although the original discrete ordinate calculations employed 51 and 171 groups, these comparison calculations were performed with only 12 groups, the energy structure for which is shown in Table 1. Note that the energy range is sufficient to encompass all threshold reaction rates measured in the PCA-PVF. Details of the generation of this cross section library are described elsewhere.[4,9] Note also that the 12-group discrete ordinate calculations described here are not in any direct way connected with the 51-group DOT calculations used in the PCA-PVF analysis by ORNL.[2-6]

TABLE 1. NEUTRON GROUP STRUCTURE AND SOURCE ENERGY DISTRIBUTION

GROUP	UPPER ENERGY (eV)	SOURCE FRACTION[a]
1	1.9640E 07	5.5841E-04
2	1.1052E 07	4.7115E-03
3	6.1873E 06	2.0686E-02
4	6.0653E 06	8.1625E-02
5	4.0657E 06	1.0943E-01
6	3.0119E 06	6.6245E-02
7	2.5924E 06	9.4196E-02
8	2.1225E 06	7.1393E-02
9	1.8268E 06	9.1620E-02
10	1.4957E 06	8.3815E-02
11	1.2246E 06	1.0632E-01
12	9.0718E 05	1.0401E-01
	6.0810E 05	

[a]DERIVED FROM THE ENDF/B-V WATT THERMAL FISSION SPECTRUM FOR ^{235}U.

Although the calculation of the denominator in Eq. (2) is one-dimensional, the use of the two-dimensional code DOT to calculate ϕ_Y by inserting appropriate reflecting surfaces is preferable to the use of a one-dimensional code for this purpose because it preserves the same angular quadrature as is used in the calculation of the numerator ϕ_{YZ}.

The PCA-PVF problem features a large neutron source volume emitting neutrons which impinge upon essentially point detectors at locations D1 through D7 in Fig. 2. The penetration distance from the core to detector

D7 is of the order of 10 mean free paths for 2 MeV neutrons. Running MORSE in the forward mode with next flight statistical estimators is prohibitively expensive without the application of sophisticated biasing techniques. The use of boundary crossing or finite detector volume estimators reduces the expense substantially, but yields troublesome averaged fluxes rather than point fluxes. On the other hand, running MORSE in the adjoint mode not only permits the use of a track length estimator which scores over the entire core volume, but also avoids the singularity and associated poor statistics inherent in a point detector estimator. The disadvantage of using the adjoint mode is that a separate calculation is required for each detector location and, for reliable statistics, for each energy group as well. However, for the PCA-PVF problem the advantages of operating in the adjoint mode far outweigh the disadvantages. Hence, operating in the adjoint mode with only standard biasing techniques (i.e., Russian roulette, splitting, and pathlength stretching) was selected as the method for calculating the three-dimensional fluxes.

RESULTS

The units chosen for the fluxes (really fluences) presented in this section are neutrons per square centimeter per source neutron emitted from a cubic centimeter of the core. This particular normalization arises naturally from the Monte Carlo scoring procedure over the core volume as well as from treating the use of infinite dimensions in the DOT calculations. Multiplication of these results by the space-averaged neutron source density (in units of neutrons per second per cubic centimeter) would yield absolute fluxes.

Before Eq. (2) was tested, the presence of any possible bias in one method relative to the other was first investigated. Both MORSE and DOT were applied to identical one-dimensional and two-dimensional problems for several detectors. Table 2 shows a comparison of the total fluxes (group fluxes summed over all twelve groups) calculated with DOT (columns two through four) and with MORSE (columns five through seven). The uncertainties in the MORSE results represent one standard deviation, and are, of course, only themselves estimates. The comparisons shown in Table 2 are consistent with the fact that roughly 2/3 of the MORSE fluxes fall within one standard deviation of the DOT results. Although there is perhaps evidence of a small but unimportant bias, Table 2 serves to validate the equivalence of the two methods and provides confidence in the three-dimensional comparisons that follow.

TABLE 2. NEUTRON FLUX COMPARISONS BETWEEN DOT-IV AND ADJOINT MORSE CALCULATIONS FOR NEUTRONS ABOVE 0.6 MeV

DETECTOR	DOT-IV FLUXES[a] ϕ_{XY}	ϕ_{YZ}	ϕ_Y	ADJOINT MORSE FLUXES[a] ϕ_{XY}	ϕ_{YZ}	ϕ_Y
D1	0.775	0.804	0.927	0.786 ± 0.6%[b]	0.815 ± 0.8%[b]	0.947 ± 1.7%[b]
D2	0.414	0.435	0.522			
D3	9.40×10^{-2}	9.96×10^{-2}	0.124		9.96×10^{-2} ± 1.9%	0.124 ± 5.8%
D4	5.96×10^{-2}	6.51×10^{-2}	8.55×10^{-2}			
D5	3.86×10^{-2}	4.51×10^{-2}	5.70×10^{-2}	3.96×10^{-2} ± 3.0%	4.35×10^{-2} ± 3.7%	6.54×10^{-2} ± 5.2%
D6	2.15×10^{-2}	2.36×10^{-2}	3.38×10^{-2}	2.27×10^{-2} ± 4.6%		
D7	1.12×10^{-2}	1.23×10^{-2}	1.82×10^{-2}	1.16×10^{-2} ± 5.6%	1.38×10^{-2} ± 7.4%	2.19×10^{-2} ± 8.3%

[a]UNITS: NEUTRONS/cm^2/(SOURCE NEUTRON/cm^3) FOR ϕ_{XY} AND ϕ_Y, AND NEUTRONS/cm^2/(0.7317 SOURCE NEUTRONS/cm^3) FOR ϕ_{YZ}.
[b]UNCERTAINTIES ARE ONE σ.

In Table 3 MORSE calculated three-dimensional total fluxes are compared with the synthesized discrete ordinate values given by Eq. (2) for each detector. The relative disagreements between the two results (MORSE-DOT/DOT) are given in the last column, along with estimates of the standard deviations of the Monte Carlo results. As indicated by this column, the disagreement between the two methods is quite small - the largest being about 5%. Furthermore, these differences do not exhibit any particular trend as a function of detector location. It is true that there is evidence of a slight bias in the synthesized flux procedure (the MORSE results are slightly larger) but it is no greater than the small bias that can be ignored in the earlier comparisons in Table 2.

TABLE 3. THREE-DIMENSIONAL FLUX COMPARISONS FOR NEUTRONS ABOVE 0.6 MeV

DETECTOR	ADJOINT MORSE[a] ϕ_{XYZ}	DOT-IV CONSTRUCTION[a] $\phi_{XY}(\phi_{YZ}/\phi_Y)$	RELATIVE ERROR (%)
D1	0.682 ± 0.5%[b]	0.672	1.5 ± 0.5[b]
D2	0.346 ± 0.8%	0.345	0.3 ± 0.8
D3	7.77×10^{-2} ± 1.1%	7.55×10^{-2}	2.9 ± 1.1
D4	4.74×10^{-2} ± 1.3%	4.54×10^{-2}	4.4 ± 1.4
D5	2.85×10^{-2} ± 2.1%	2.81×10^{-2}	0.7 ± 2.1
D6	1.58×10^{-2} ± 3.4%	1.50×10^{-2}	5.3 ± 3.6
D7	7.53×10^{-3} ± 3.5%	7.57×10^{-3}	−0.5 ± 3.5

[a]UNITS: neutrons/cm^2/(source neutron/cm^3).
[b]UNCERTAINTIES ARE ONE σ.

Calculated one-and two-dimensional group fluxes using DOT are shown in Table 4 for detector D5 which corresponds to the "T/4" location. A summation over groups of these fluxes would yield the total flux values

for detector D5 in Table 2. The DOT fluxes from Table 4 are then combined using Eq. (2) to form the various group fluxes which are then com-

TABLE 4. DOT-IV NEUTRON GROUP FLUXES AT DETECTOR D5

ENERGY GROUP	DOT-IV FLUXES[a] ϕ_{XY}	ϕ_{YZ}	ϕ_{Y}
1	2.17×10^{-5}	2.23×10^{-5}	3.15×10^{-5}
2	1.41×10^{-4}	1.45×10^{-4}	2.10×10^{-4}
3	4.77×10^{-4}	4.95×10^{-4}	6.72×10^{-4}
4	1.31×10^{-3}	1.38×10^{-3}	1.83×10^{-3}
5	1.42×10^{-3}	1.51×10^{-3}	1.98×10^{-3}
6	1.37×10^{-3}	1.46×10^{-3}	1.93×10^{-3}
7	2.69×10^{-3}	2.87×10^{-3}	3.79×10^{-3}
8	1.99×10^{-3}	2.13×10^{-3}	2.82×10^{-3}
9	3.55×10^{-3}	3.81×10^{-3}	5.08×10^{-3}
10	3.82×10^{-3}	4.10×10^{-3}	5.47×10^{-3}
11	7.38×10^{-3}	7.98×10^{-3}	1.09×10^{-3}
12	1.44×10^{-2}	1.56×10^{-2}	2.21×10^{-2}

[a]UNITS: neutrons/cm^2/(SOURCE neutron/cm^3) FOR ϕ_{XY} AND ϕ_{Y}, AND neutrons/cm^2/(0.7317 SOURCE neutron/cm^3) FOR ϕ_{YZ}.

pared with the MORSE results in Table 5. (The summation over groups of the synthesized group fluxes appearing in Table 5 is the value 2.81×10^{-2} for detector D5 shown in Table 3). The synthesized group

TABLE 5. THREE-DIMENSIONAL GROUP FLUX COMPARISONS AT DETECTOR D5

ENERGY GROUP	ADJOINT MORSE[a] ϕ_{XYZ}	DOT-IV CONSTRUCTION[a] $\phi_{XY}(\phi_{YZ}/\phi_{Y})$	RELATIVE ERROR (%)
1	$1.56 \times 10^{-5} \pm 3.0\%$[b]	1.54×10^{-5}	1.3 ± 3.0[b]
2	$1.04 \times 10^{-4} \pm 1.9\%$	1.02×10^{-4}	2.0 ± 1.9
3	$3.62 \times 10^{-4} \pm 3.5\%$	3.51×10^{-4}	3.1 ± 3.6
4	$9.97 \times 10^{-4} \pm 2.9\%$	9.88×10^{-4}	0.9 ± 2.9
5	$1.07 \times 10^{-3} \pm 3.7\%$	1.08×10^{-3}	-0.9 ± 3.7
6	$9.83 \times 10^{-4} \pm 3.6\%$	1.04×10^{-3}	-5.5 ± 3.4
7	$1.99 \times 10^{-3} \pm 2.4\%$	2.04×10^{-3}	-2.4 ± 2.3
8	$1.44 \times 10^{-3} \pm 2.3\%$	1.50×10^{-3}	-4.0 ± 2.2
9	$2.79 \times 10^{-3} \pm 2.5\%$	2.66×10^{-3}	4.9 ± 2.6
10	$2.69 \times 10^{-3} \pm 2.3\%$	2.86×10^{-3}	-5.9 ± 2.2
11	$4.88 \times 10^{-3} \pm 2.4\%$	5.40×10^{-3}	-9.6 ± 2.2
12	$9.60 \times 10^{-3} \pm 2.2\%$	1.02×10^{-2}	-5.9 ± 2.1

[a]UNITS: neutrons/cm^2/(source neutron/cm^3).
[b]UNCERTAINTIES ARE ONE σ.

fluxes compare well with the MORSE fluxes for the first nine groups (E>1.5MeV), but there is an indication of a small disagreement outside of statistics for the synthesized group fluxes between 0.6 and 1.5 MeV. However, this latter disagreement is still probably due to statistical fluctuations since the total fluxes shown in Table 3 are in agreement when based on an earlier MORSE result.

CONCLUSIONS

Recalling that the object of this study was an evaluation of the accuracy of the flux synthesis method combining the results of three discrete ordinates calculations represented by Eq. (2), the investigations of the previous section clearly validate the use of this approximation over the PCA-PVF space and energy domain studied (i.e., over all y in the 8/7 configuration for x=z=0 and E>0.6 MeV). Based on this conclusion, use of Eq. (2) for somewhat less restrictive domains of x,y, and z and E is most likely justified. In particular, it should apply to the centerline threshold detectors in the 12/13 configuration.

It should further be noted that the combined three-dimensional aspects of the PCA-PVF geometry and source distribution apparently are separable and cancel out using the DOT synthesis of Eq. (2). Hence, the conjecture that any discrepancy between the PCA-PVF measurements and ORNL calculations is most likely due to the neglect of three-dimensional coupling effects, implied by Eq. (2), is shown to be unfounded by the results of this study. Apparently, the source of this discrepancy lies elsewhere.

REFERENCES

1. W. N. McElroy et. al., "LWR Pressure Vessel Surveillance Dosimetry Improvement Program," HEDL SA-1949, Proc. of NRC Seventh Water Reactor Safety Research Information Meeting in Gaithersburg, Maryland, Nov. 5-9, 1979.

2. F. W. Smallman, F. B. K. Kam, J. F. Eastham, and C. A. Baldwin, "Reactor Calculation 'Benchmark' PCA Blind Test Results," ORNL/NUREG/TM-428, Oak Ridge National Laboratory (1981).

3. W. N. McElroy, editor, "LWR Pressure Vessel Surveillance Dosimetry Improvement Program: PCA Experiments and Blind Test," NUREG/CR-1861 HEDL-TME 80-87, R5 Hanford Engineering Development Laboratory (1981).

4. R. E. Maerker, J. J. Wagschal, and B. L. Broadhead, "Development and Demonstration of an Advanced Methodology for LWR Dosimetry Applications," EPRI NP-2188 Project 1399-1 Interim Report (1981).

5. R. E. Maerker, "S_n Transport Calculations of the PCA Experiments with Some Estimated Uncertainties," Trans. Am. Nucl. Soc. 34, 628 (1980).

6. J. J. Wagschal, R. E. Maerker, and B. L. Broadhead, "LWR-PV Damage Estimate Methodology," Proceedings of the Conference 1980 Advances in Reactor Physics and Shielding, Sept. 14-17, Sun Valley, Idaho, pp. 612-624 (1980).

7. M. B. Emmett, "The MORSE Monte Carlo Radiation Transport Code System," ORNL-4972, Oak Ridge National Laboratory (1975).

8. W. A. Rhoades, D. B. Simpson, R. L. Childs, and W. W. Engle, "The DOT-IV Two Dimensional Discrete Ordinates Transport Code with Space-Dependent Mesh and Quadrature," ORNL/TM-6529, Oak Ridge National Laboratory (1979).

9. R. E. Maerker and P. J. Maudlin, "Supplementary Neutron Flux Calculations for the ORNL Pool Critical Assembly Pressure Vessel Facility," ORNL/TM-7602, Oak Ridge National Laboratory (1981).